

Biases of a ring-image turbulence sensor

Authors: *A. Tokovinin*

Version: 2

Date: 2020-09-10

File: prj/smss/doc/ring-biases.tex

1 Software tools

In this document, I study the reaction of a turbulence sensor based on a ring-like image, RINGSS, to various deviations from its ideal or assumed parameters, for example a coma aberration. I use end-to-end simulations and an analytic calculation of weighting functions. Unless specified otherwise, the instrument parameters are: telescope diameter $D = 0.13$ m, central obscuration $\epsilon = 0.5$, wavelength $\lambda = 0.6$ μm , monochromatic light.

The end-to-end simulation uses `simatm.pro` that generates a Kolmogorov phase screen, propagates it over a certain distance z (for monochromatic light) and saves the resulting complex light amplitude. I used 2.5-mm grid step and 1024^2 grid. The second code `ringsim.pro` “drags” these amplitude screens in front of the telescope aperture and computes the resulting cube of ring-like monochromatic images. The defocused ring-like images are produced by summing Zernike aberrations (defocus and spherical) with phase at the pupil. Here I use Zernike polynomials in the Noll’s notation and express their coefficients in radians at wavelength λ ; these standard full-aperture polynomials ignore the central obscuration (lack of ortho-normality is not an issue here). Defocusing the telescope to a virtual conjugation altitude H (negative for intra-focal images considered here) corresponds to the Zernike defocus coefficient

$$a_4 = \frac{\pi D^2}{16\sqrt{3}\lambda H}. \quad (1)$$

The matching spherical aberration needed to produce an almost conic wavefront (hence a sharp ring) is $a_{11} = -0.1a_4$, according to the FADE prescription for obtaining approximately conic wavefront shape. Optionally, an arbitrary number of other Zernike aberrations can be added to simulate de-center, coma, etc. Noise is not simulated so far. The simulated image cube is processed by the standard tools `cubecoef.pro` and `statmom.pro`. The angular power spectrum $S(m)$ is converted into a weighting function (WF) $W(m) = S(m)/J$ after its division by the simulated turbulence integral J .

The analytical weight calculator `aweight2.pro` is described elsewhere. Here, polychromatic WFs are computed in the small-signal approximation. The telescope pupil is an annulus with phase aberrations corresponding to a_4 and a_{11} with an optional addition of other Zernike terms.

2 Ring radius

First, a relation between the radius of the ring-like image and the defocus H is established. The nominal angular ring radius R_{geom} is computed as the average wavefront radial tilt inside the annulus,

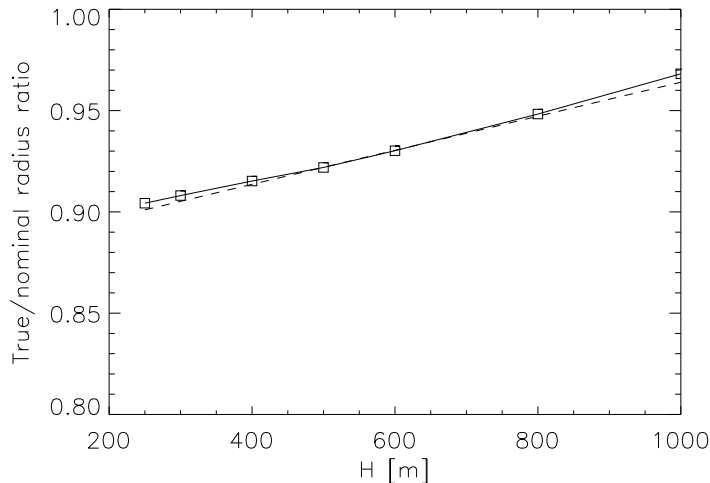


Figure 1: Ratio of true (diffraction) and nominal (geometric) ring radii vs. conjugation distance H . The dashed line is a linear approximation.

it equals

$$R_{\text{geom}} = D(1 + \epsilon)/(4H). \quad (2)$$

The actual image radius computed by `getimage.pro` using physical optics R_{phys} is slightly less (Fig. 1), partly because the spherical aberration, applied jointly with defocus, slightly reduces the overall radial wavefront gradient. The ratio differs from one only within 10% and depends slightly on H ; a linear fit is $R_{\text{phys}}/R_{\text{geom}} \approx 0.88 + 0.000085H$, where H is in meters. This ratio also depends on the central obscuration ϵ . Knowing the measured ring radius, we can accurately calculate the actual conjugation distance.

3 Conjugation distance bias

Mismatch between actual and assumed conjugation distances translates into the difference between actual and assumed WFs and, therefore leads to a bias. This bias is not important because the actual value of H is known from the ring radius (see above). Nevertheless, it is useful to evaluate the impact of a wrong H .

The WF ratio was computed by the code `hbias` in `biases.pro` using the instrument parameters in `sim1.par` but with a real polychromatic response to a star with effective temperature of 6000 K (code `aweight2.pro`). The results are plotted in Fig. 2. At moderate and small frequencies, e.g. $m = 5$, the effect at small z is as expected: larger response for a larger conjugation distance, hence smaller rings. At larger m this monotonic behavior is no longer valid, and the WF bias can be either positive or negative. However, even for a relatively large discrepancy in H the bias remains commensurable with the discrepancy itself, i.e. within 20%. I conclude that moderate mismatch between actual and assumed conjugation distances is tolerable. Note that this mismatch is irrelevant at large z . The

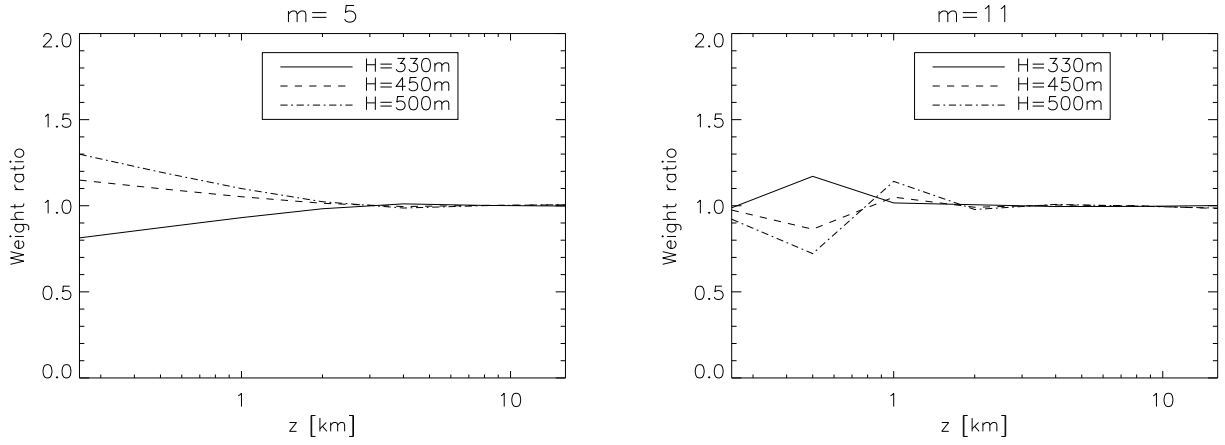


Figure 2: Ratio of WF at a given conjugation distance H to the WF at nominal $H = 400$ m.

experimental data show remarkably little change of the APS when the telescope is refocused and the ring radius varies by a substantial factor, up to two.

4 Coma bias

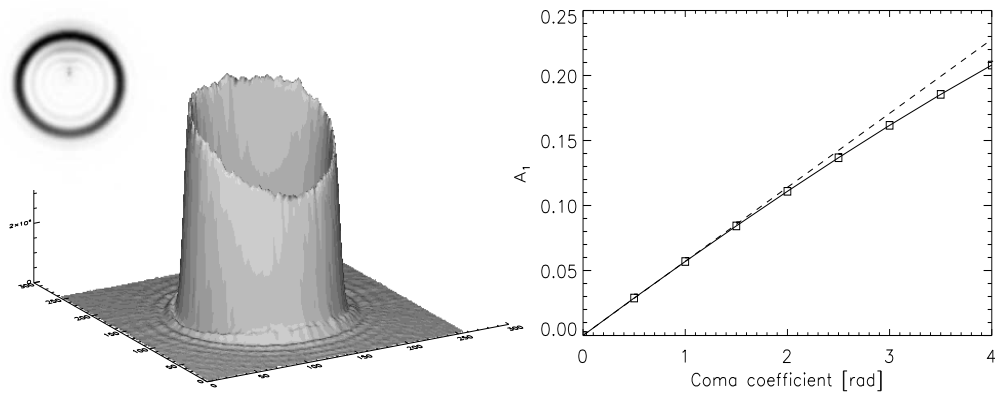


Figure 3: Ring image corresponding to coma aberration of 2 rad. The plot on the right shows relation between ring asymmetry index A_1 and Zernike coma coefficient a_7 . The dashed line is a linear relation with a slope of 0.057.

Coma aberration distorts the image and, at the same time, displaces its centroid. To compensate for the shift, I apply the coma coefficient a_7 jointly with the tilt corrector $a_3 = -4a_7$ (however, the rings are re-centered anyway during processing). I found that such correction leaves the ring approximately centered. Figure 3 illustrates distortion of the ring-like image by $a_7 = 2$ rad ($\lambda/3$ rms wavefront deviation). The asymmetry of azimuthal intensity distribution in the ring is quantified by

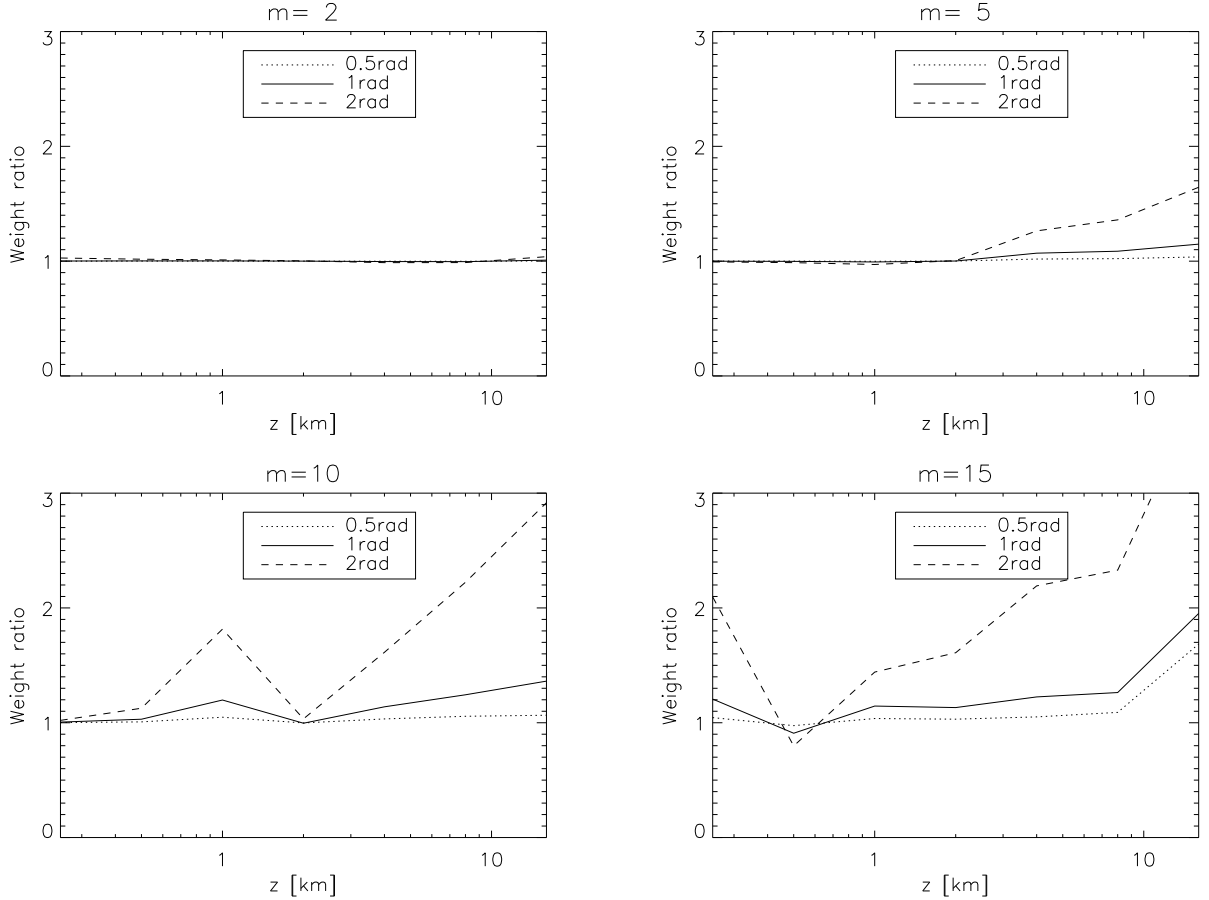


Figure 4: WF bias caused by the coma aberration at frequencies $m = 2$, $m = 5$ (top) and $m = 10$, $m = 15$ (bottom).

the amplitude of the average $m = 1$ coefficient, $A_1 = \sqrt{c_1^2 + s_1^2}$. The asymmetry index was computed for several values of a_7 , and the resulting plot shows that the relation between A_1 and a_7 is linear with a slope of 0.057.

Analytic evaluation of the coma-induced bias was made using `comabias` in `biases.pro`. Polychromatic WFs for a star with effective temperature of 6000 K are computed using `aweight2.pro` for the coma coefficient of 0.5, 1, and 2 radian (at 600 nm). Figure 4 shows representative results. Almost no bias is found at low frequencies, only a modest bias at $m = 5$, and an increasingly large bias at larger m . However, at large m the WFs substantially differ from zero only at small z , while the relative bias increases with z . Figure 5 illustrates this point by plotting the WFs on linear scale.

This study shows that a coma aberration of 1 radian (or $A_1 = 0.06$) has little effect on the WFs, hence it is not expected to bias the results, but a larger coma, obvious by the ring distortion it produces, should be avoided. The pipeline computes and stores the A_1 parameter (coma amplitude), providing quantitative control of the optical alignment.

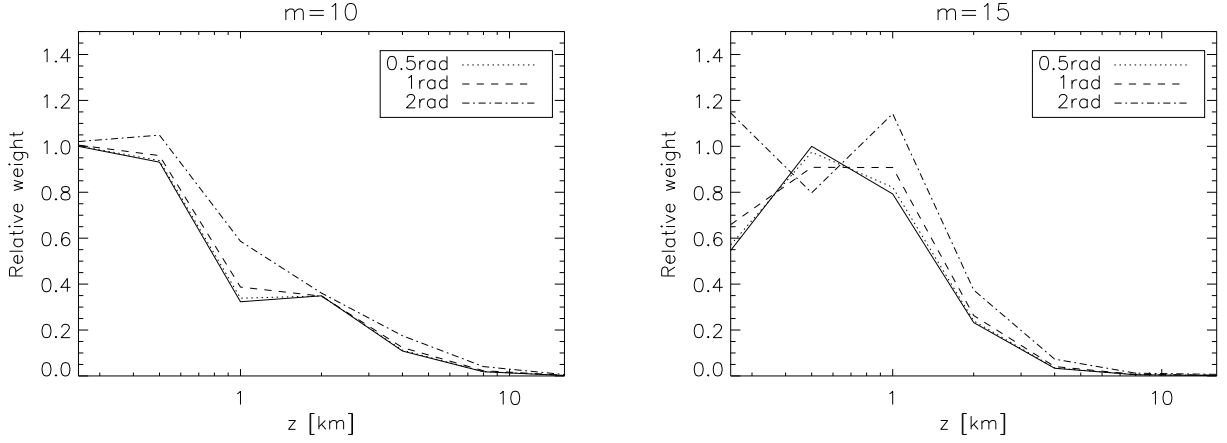


Figure 5: Relative WFs on the linear scale and their bias induced by coma for $m = 10$ and $m = 15$. Solid line show the nominal (undistorted) WFs.

5 Aperture geometry

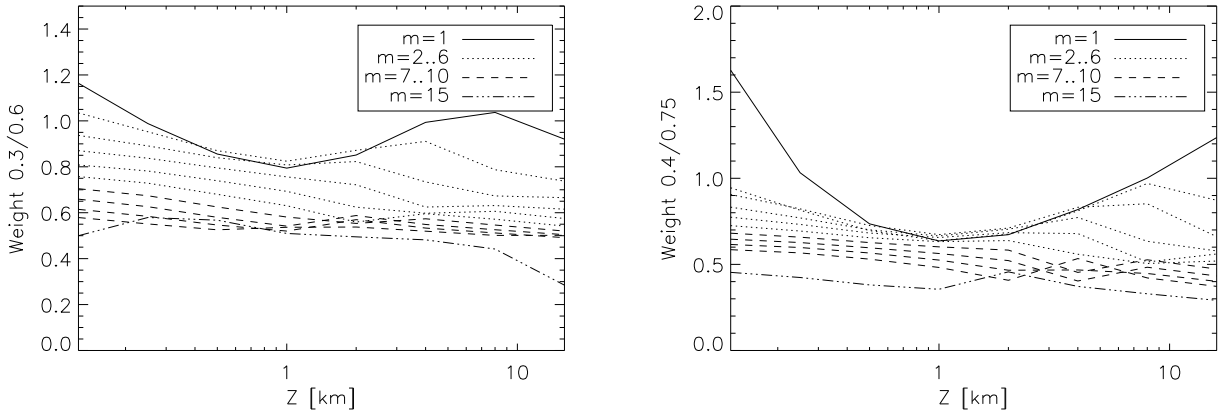


Figure 6: Influence of the central obscuration ϵ on the WFs. Left: WF ratio for wide/narrow annuli, $\epsilon = 0.3/0.6$, and $D = 0.13$ m. Right: same comparison for $D = 20$ cm and $\epsilon = 0.4/0.75$.

Next, I study dependence of the WFs on the aperture geometry, namely the aperture diameter D and the width of the annulus (i.e. on ϵ). One expects that mixing light from a wider annulus in the ring image would reduce the amplitude of small-scale scintillation signal, i.e. would give smaller WFs for large m and/or at small z . Figure 6 confirms these expectations. However, the loss of scintillation signal is almost entirely compensated by increase of the photon flux in a larger annulus. This is further elaborated in `datproc.pdf` where the signal to noise plots are given.